ANALYSIS OF AN AIRCRAFT CARGO NET BARRIER USING MSC/NASTRAN

Adrian Viisoreanu, Ph.D., Alexander Rutman, Ph.D., Gary Cassatt, M.S.

Boeing Commercial Airplane Group
P.O. Box 7730, MS K01-11
Wichita KS 67277-7730

ABSTRACT

Aircraft cargo net barriers are designed to arrest the cargo and protect the cabin crew during a survivable crash landing. Compared with metallic or composite aircraft structures, cargo nets are extremely flexible and develop large displacements under loading, making their behavior predominately non-linear and creating convergence problems. This paper presents modeling techniques and cargo net analysis strategy for MSC/NASTRAN solution 106. Parametric studies address the influence of the net initial shape and net - cargo interaction under crash landing conditions.

INTRODUCTION

The cargo net barrier and its fittings are airworthiness items. Their function is to arrest the cargo and protect the cabin crew during a crash landing. By FAA regulation, the cargo barrier must sustain a 9g inertia load applied as a static load (Figure 1).

The purpose of this study is to establish finite element modeling techniques and a cargo net analysis strategy. The main goal of the analysis was to determine the cargo net fitting reactions, strains in the net straps, and the net deformed shape. The investigation was performed using MSC/NASTRAN non-linear solution 106 with large displacements.

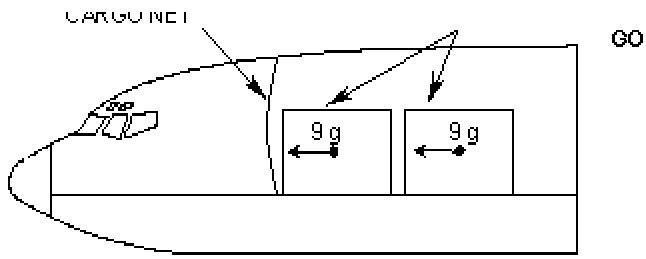

Figure 1. Cargo Net Functional Schematic

The cargo net analyzed in this study was made from radial and circumferential straps. Under crash loads, the cargo net deforms approximately as a membrane under pressure. The net straps are made from woven DACRON fibers and have practically no bending stiffness. When crash loads are applied the net behaves as a mechanism until it reaches an equilibrium position, reacting the loads by tension in the radial straps.

When the cargo net is in equilibrium with the external loads it becomes quite stiff and stable. However, the net is initially very flexible and creates convergence problems in the analysis. A special strategy was developed to alleviate this problem.

At the first moment the cargo net has an initial deflection determined only by the length of the straps and it is impossible to know its exact initial shape. Parametric studies were conducted to show the influence of the net initial shape and initial deflection on its final shape and fitting reactions.

The influence of the net loading on its final shape and reactions was also investigated. Depending on the kind of cargo carried, the applied loads could range from a uniformly distributed pressure following the net deformed shape (follower pressure) to a forward force parallel with the aircraft longitudinal axis during the load cycle.

FINITE ELEMENT MODEL

ELEMENTS AND MATERIALS

The finite element model (FEM) of the cargo net consists of radial straps, circumferential straps, and a non-structural membrane (Figure 2). The aft ends of the radial straps attach to the fuselage fittings with metallic links. A fiberglass ring connects the forward ends of the radial straps. The fittings follow the fuselage outline, except for the lower attach points that are on the main cargo deck floor.

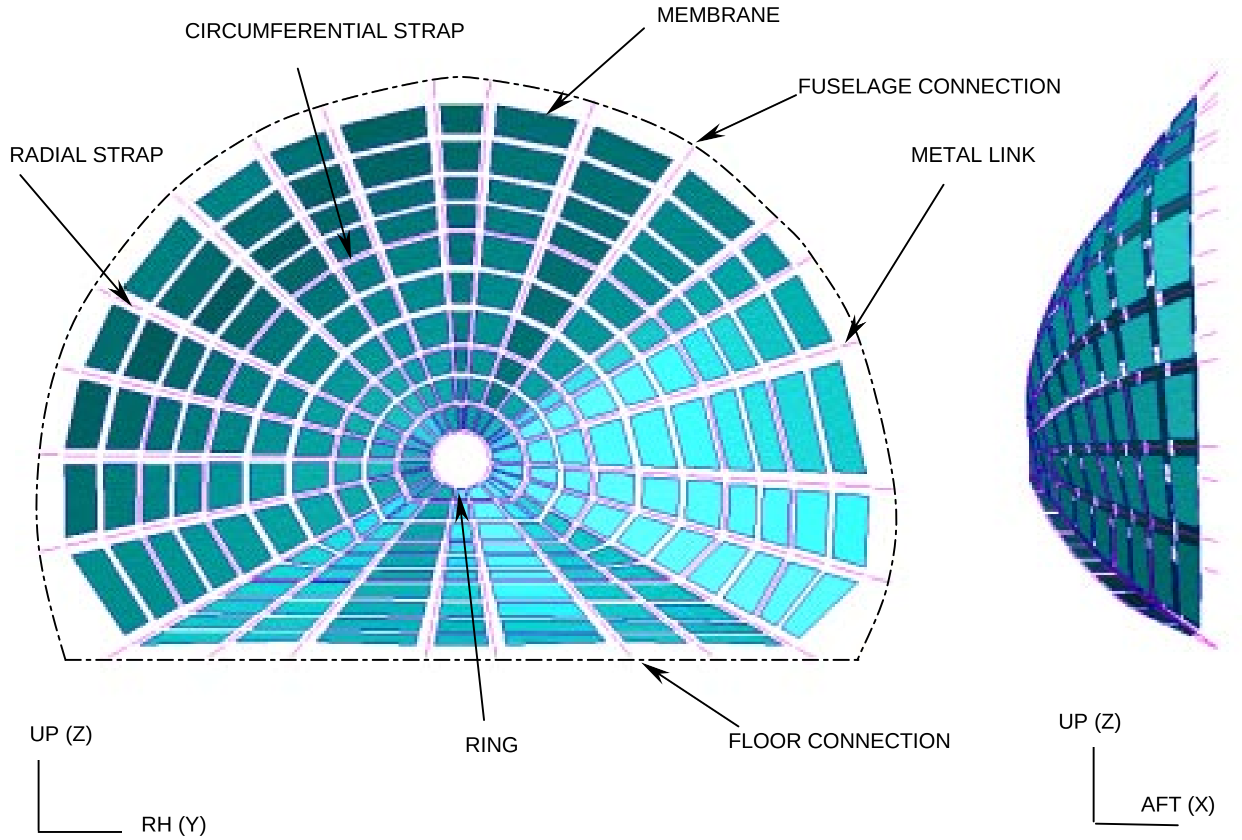

Figure 2. Cargo Net Barrier Finite Element Model

The initial shape of the radial straps is a circle arc. The radial straps were modeled by CBEAM elements with their actual cross sectional area, but very small dummy moments of inertia.

The small values of the area moments of inertia and torsional constant do not influence the final results, but are important to assure the model stability at the beginning of the loading cycle, when the applied load is extremely small and the net is not in equilibrium.

The radial strap material follows a non-linear stress strain function derived from experimental Load - Elongation curves for MIL-W-25361 Polyester Webbing (DACRON). Although the straps are loaded in tension, a small compressive stiffness was assumed to stabilize the model at the beginning of the load cycle. The circumferential straps were modeled by CROD elements made from the same material as the radial straps.

In two of the load cases considered, a uniform pressure was applied to the cargo net to simulate the crash loads. The purpose of the membrane is to distribute the applied pressure to the strap nodes. The membrane was modeled with CQUAD4 elements, made from the same material as the straps, 0.0001 inch thick.

The membrane elements react the applied pressure as concentrated loads at their corners. If the membrane element has a common node with the attach fittings, it introduces a fictitious force at the fitting, perpendicular to the plane of the membrane and dependent on the area of the CQUAD4 element. To circumvent this problem the membrane elements from the outer row were removed (Figures 3 and 4).

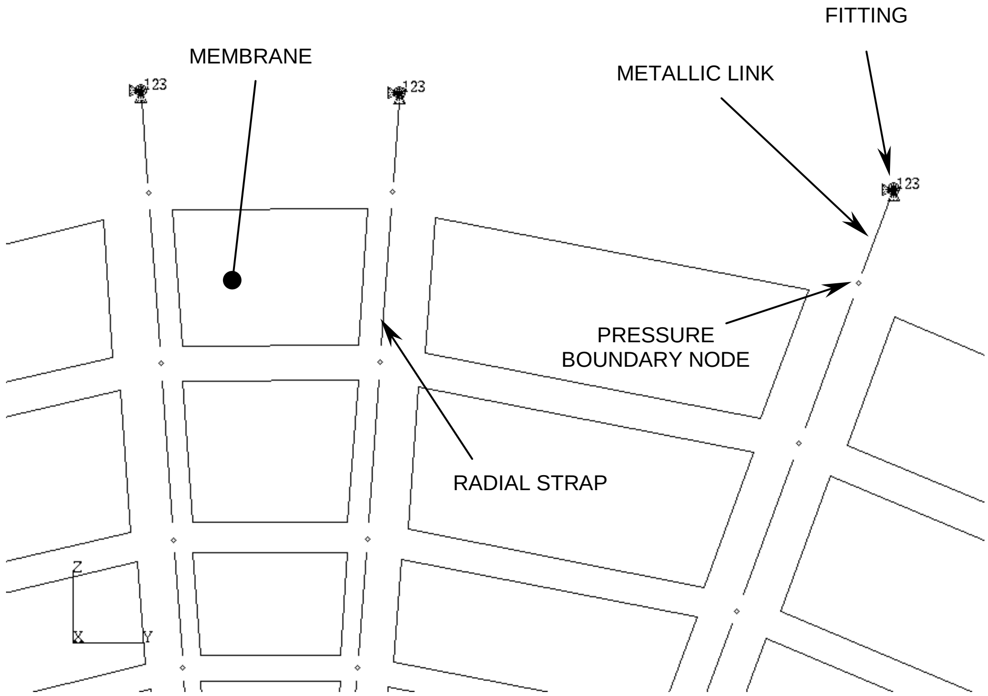

Figure 3. Model of Fuselage Attachment

The metallic links were modeled by CBEAM elements made from a 2024-T3 bar. The length of the metallic links was adjusted such that the pressure boundary nodes lay in a plane perpendicular to the longitudinal axis (X) at the end of the loading cycle (Figure 4). Otherwise the resultant of the applied pressure will not be parallel to the longitudinal axis (X).

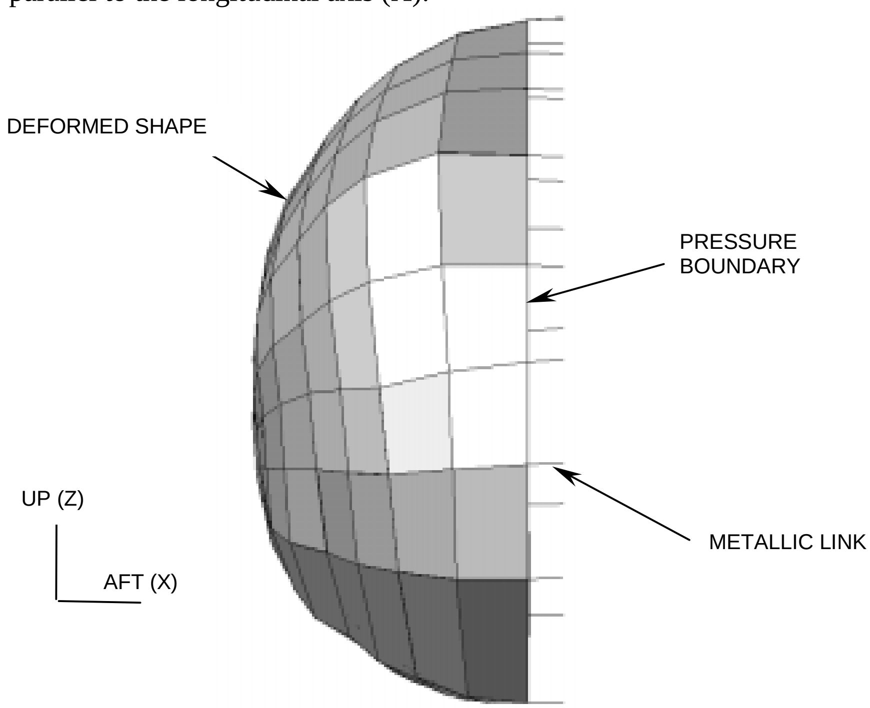

Figure 4. Pressure Boundary of Deformed Net

The links attached to the fuselage are almost parallel to the fuselage stringers when the net is loaded so they all have the same length. After deformation the links attached to the cargo floor make different angles with the longitudinal axis and their length was calculated for each individual link (Figure 5).

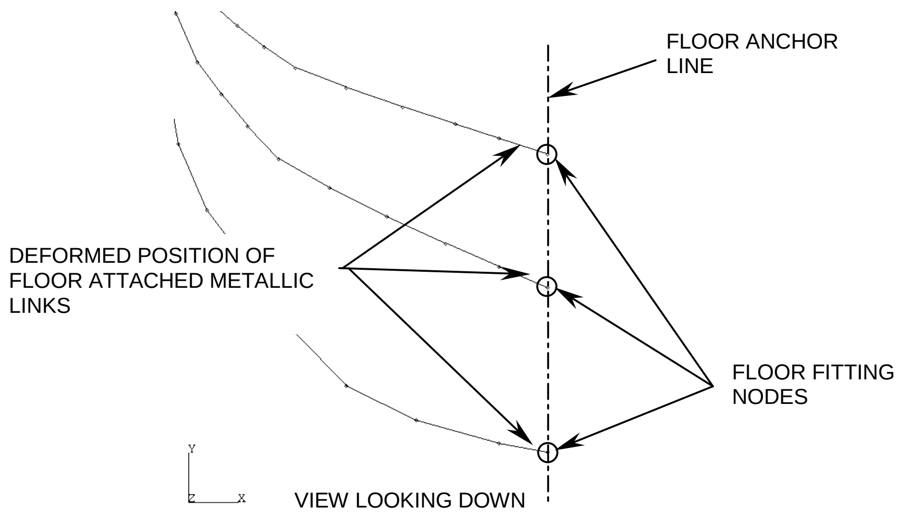

Figure 5. Deformed Shape of Floor Links

CONSTRAINTS

The translational degrees of freedom (DOF) were constrained at the nodes representing the fuselage and floor attachment fittings (Figure 6).

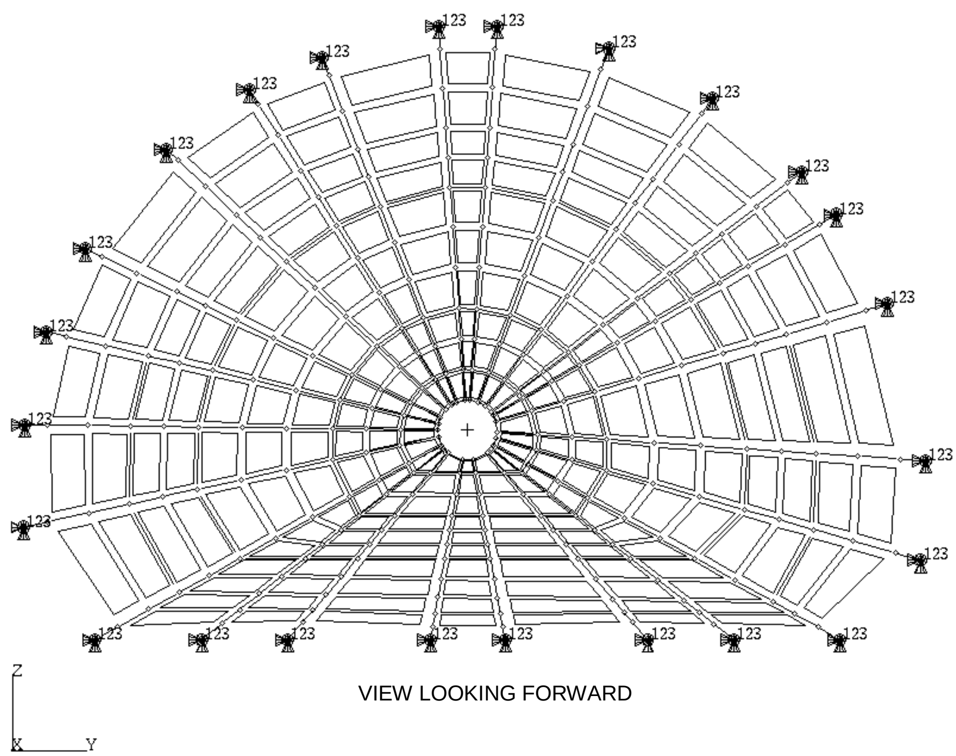

Figure 6. Fuselage Fittings Constraints

Under maximum pressure loads, part of the net comes in contact with the fuselage shell and the floor. To model the net to fuselage contact, slide lines were at each of the fuselage fittings. The properties of the slide lines were:

Stiffness Scaling Factor (SFAC) = 1 (default)
Slide Line Width (W1) = 20 in
Coefficient of Static Friction (MU1) = 0

Two non-structural nodes defined the master line. Since the AUTOSPC parameter does not work in the non-linear solution, all DOF's of the non-structural nodes were constrained. The master line could be defined using the fuselage fitting node, but since separate reactions for the fitting and fuselage contact were required, a non-structural node was created at 0.1 inch in front of the fitting node (Figure 7).

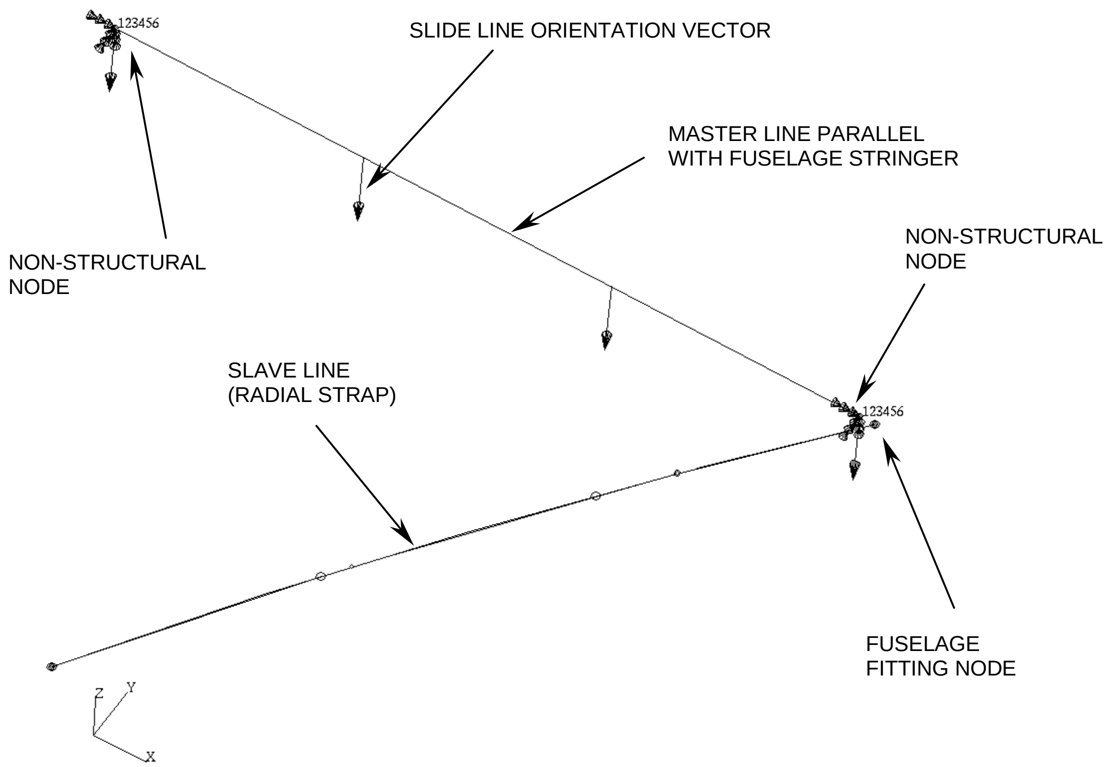

Figure 7. Slide Line along Fuselage Stringers

Because the links attached to the floor are not parallel with the longitudinal axis, slide lines on the floor would react a longitudinal component of the contact load (Figure 8). Such a model would not correctly represent the actual interaction between net and floor.

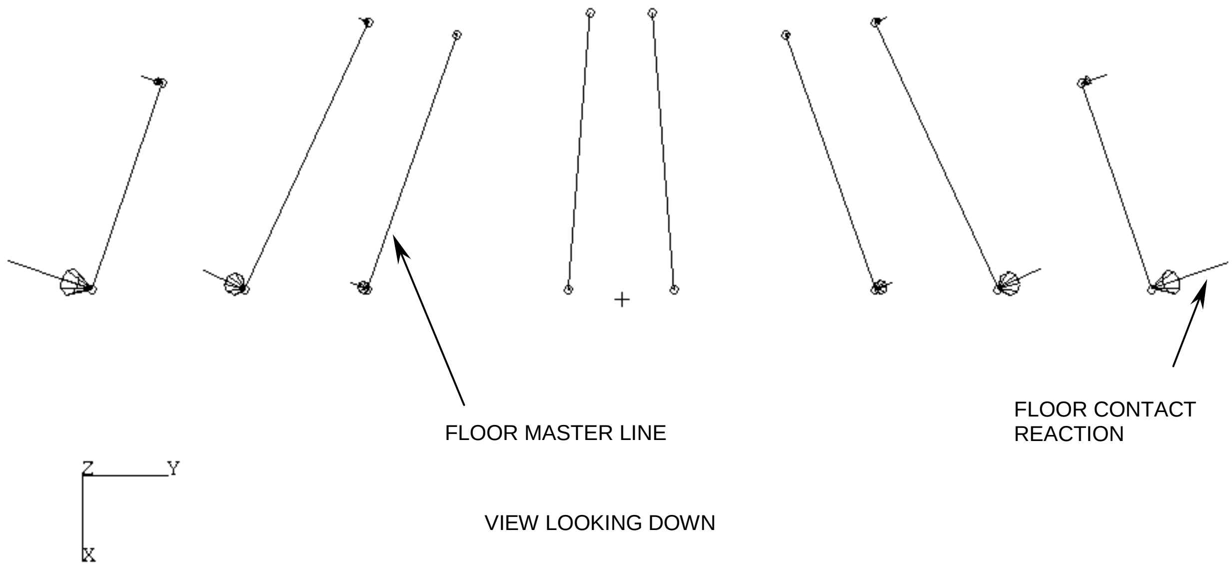

Figure 8. Floor Master Lines React Longitudinal Component

Making the floor master slide lines parallel with the longitudinal axis would eliminate the longitudinal component of the contact reaction. However, in this case the contact elements on the floor would not close.

To model the contact between the net and the floor, CGAP elements were used. The upper node of the gap element was on the radial strap and the other node on the floor (Figure 9). Preliminary analysis showed only the first two nodes of the radial strap came in contact with the floor. The floor nodes are non-structural and have all DOF's constrained. The properties of the gap elements are:

Gap Orientation: Coordinate 1
Initial Gap Opening: Distance between initial position of strap node and floor plane
Closed Stiffness: 100,000 psi
Maximum Penetration: 0.001

The radial strap does not move straight towards the floor, but also rotates about a vertical axis passing through the fitting node. The gap element orientation was given by axis X of coordinate system 1. This made the MSC/NASTRAN program evaluate only the vertical separation between the strap node and the floor plane, rather than the total distance between the two nodes of the gap element.

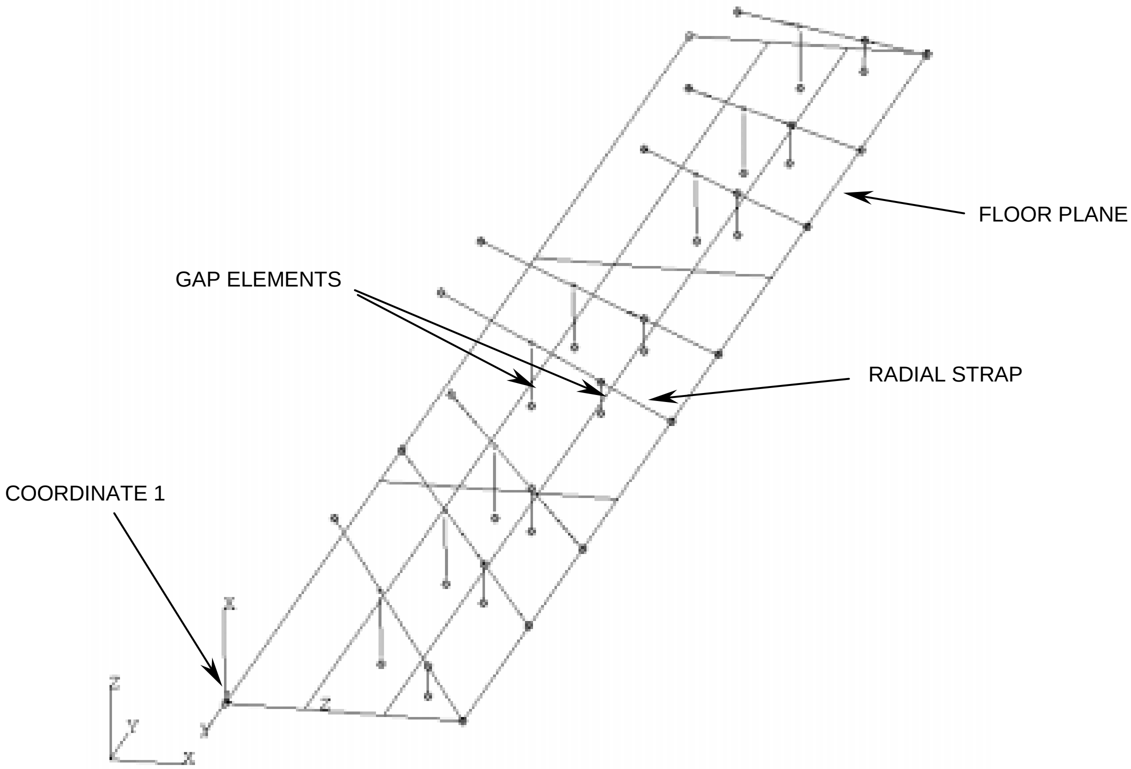

Figure 9. Floor Gap Elements

<u>LOADS</u>

Three types of applied loads were considered: (a) uniformly distributed pressure, (b) force parallel to the aircraft longitudinal axis, and (c) combination of pressure and axial force. The cargo net load depends on the cargo carried. If small parcels predominate, the load distribution would be similar to hydrostatic pressure and the uniform pressure would be representative. In the case of a heavy and hard parcel (i.e. an engine), the longitudinal force would be more representative. The combination of pressure and longitudinal force is a mix of the two extreme load configurations that is representative for most common cargo mixes.

Uniformly Distributed Pressure

The pressure uniformly distributed on the net was represented by PLOAD4 follower pressure applied to the membrane elements and FORCE2 follower forces acting on the central ring (Figure 10).

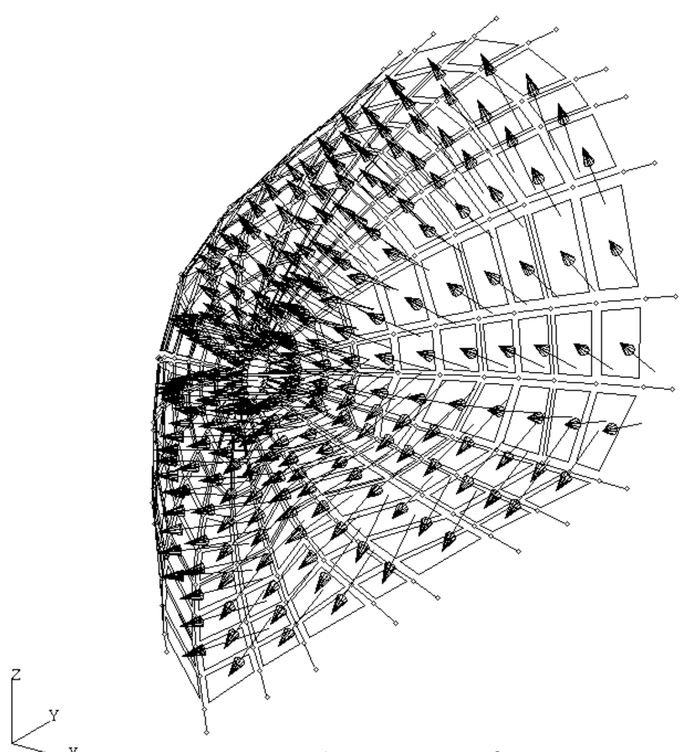

Figure 10. Uniform Pressure

The membrane did not cover the central ring. The load corresponding to the area of the ring was applied as a uniformly distributed force along the circumference of the ring. FORCE2 was used to make this load a follower force normal to the plane of the ring during the load cycle. The nodes used to define the direction of FORCE2 were located on two approximately perpendicular diameters of the ring circle. Their cross product defines a vector perpendicular to the plane of the ring pointing in the forward direction.

Force Parallel with Longitudinal Axis (X)

The longitudinal forces at each node were output by MSC/NASTRAN as applied loads (OLOAD) from a flat model of the net. The flat model was constructed projecting all nodes to the plane of the fittings. The longitudinal force is non-follower and remains parallel with the aircraft longitudinal axis during the net deformation (Figure 11).

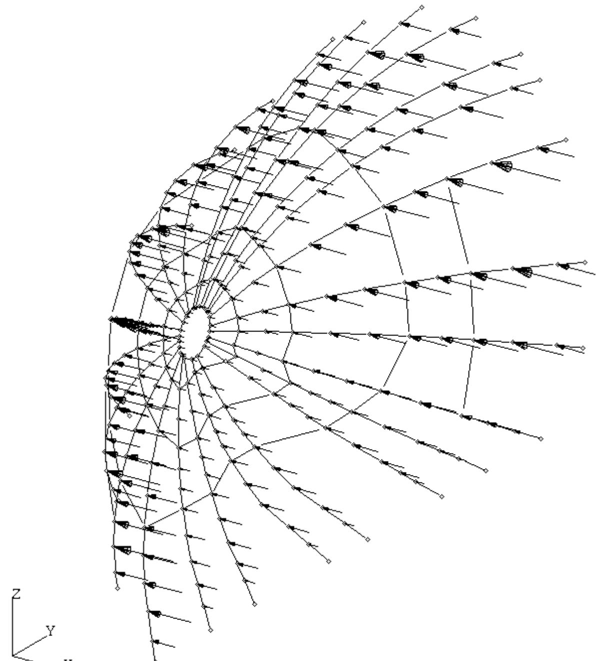

Figure 11. Longitudinal Force

Uniformly Distributed Pressure and Longitudinal Force Combination

This load case is a 50/50 linear combination of the previous two (Figure 12).

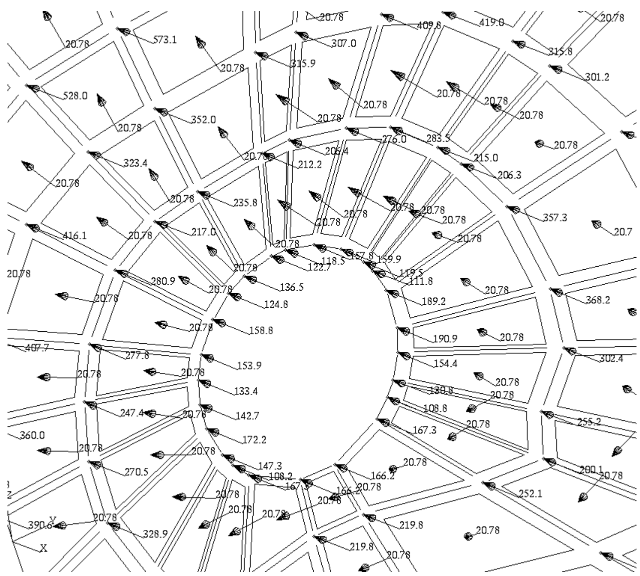

Figure 12. Longitudinal force and Uniform Pressure Combination

LOADING SEQUENCE AND CONVERGENCE CRITERIA

The cargo net problem can only be solved using a non-linear approach (MSC/NASTRAN solution 106). The large displacements of the net under increasing loads are the driving factor. The initial stiffness of the net is very small and creates convergence problems. To obtain a solution it is necessary to gradually increase the applied load starting from an extremely small value and to relax the convergence criteria at the beginning of the load cycle.

The main purpose of the first loading phase is to let the net work as a mechanism with minimal stiffness and find its own equilibrium shape under the applied loads. The first load cases were 1.E-6, 1.E-4, 1.E-2, and 1psi. The convergence was difficult during this phase because of the (a) very low stiffness of the net, and (b) initially the net was not in equilibrium with the applied loads. To alleviate this problem only the displacement error was checked and the convergence criteria in MSC/NASTRAN solution 106 were relaxed.

After the applied pressure increased to 1 psi the model became stable and converged without problems. The load error check was introduced, but the convergence accuracy was kept at 1.E-2 to save computing time. The accuracy was reset to the default 1.E-3 for the last load case. Table 1 shows the loading sequence and convergence criteria for the uniform pressure load case. The other two load cases follow a similar pattern.

Applied Pressure (psi)	Iterations	Convergence Error	
		Displacement	Load
1.00E-06	20	1.00E-01	Off
1.00E-04	20	1.00E-02	Off
1.00E-02	20	1.00E-02	Off
1	50	1.00E-02	Off
10	20	1.00E-02	1.00E-02
20	20	1.00E-02	1.00E-02
30	20	1.00E-02	1.00E-02
40	20	1.00E-03	1.00E-03

Table 1. Loading Sequence and Convergence Criteria for Uniform Pressure

ANALYSIS

This section describes the influence of the net initial shape, initial deflection, and loading scenarios on the net final deflection and fuselage fitting reactions.

INFLUENCE OF INITIAL SHAPE

To investigate the influence of the net initial shape three models were analyzed. In all cases the central ring distance to the plane of the fittings was 30 inch, but its position along the Z axis varied as shown in Table 2.

Shape	Central Ring Position (% Z_{max})
1	64
2	48
3	36

Table 2. Position of Central Ring along Z axis

As shown in Figure 13, the initial shape of the net has little influence on its final shape. There are some small variations, but the final deformed shapes are almost identical. The fitting reactions also show little change with the initial shape of the net. This eliminated the concern about the initial shape of the net that is difficult to control and allowed us to assume an initial shape made from circle arcs. The only important factor is the length of the straps.

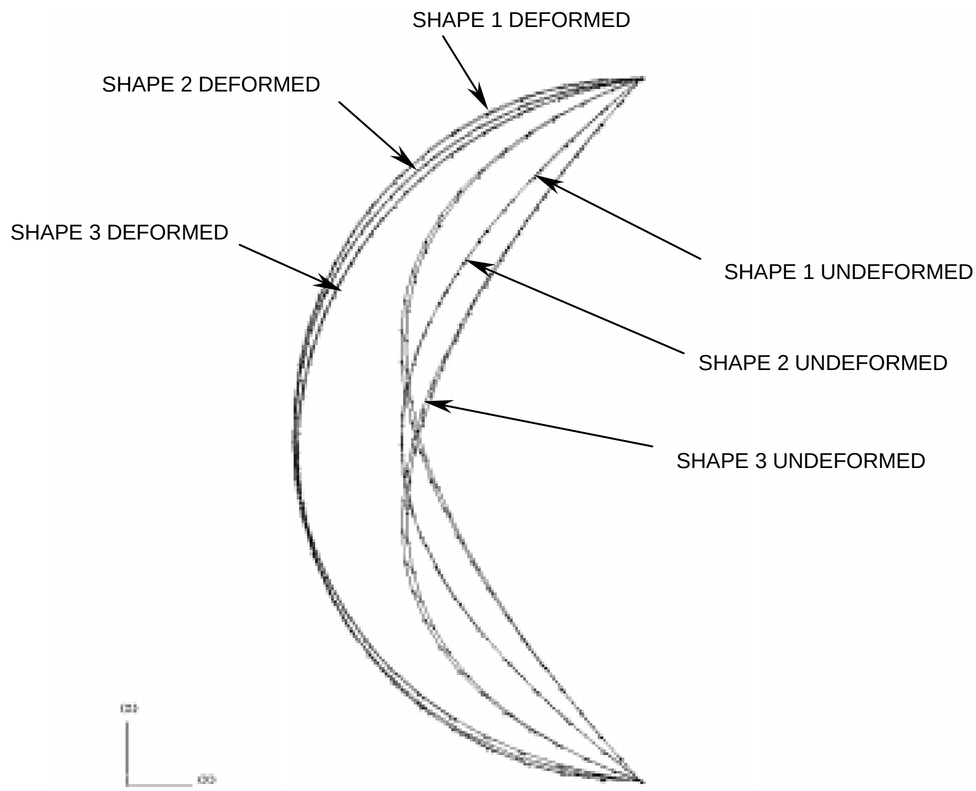

Figure 13. Influence of Net Initial Shape

<u>INFLUENCE OF INITIAL DEFLECTION</u>

Two net models (Figure 14) were analyzed to determine how the initial distance between the central ring and the plane of the fittings influences the deformed shape and fitting reactions. MODEL 30 has longer radial straps and an initial deflection of 30 inch. MODEL 15 has shorter radial straps and a 15 inch initial deflection. The same uniform distributed pressure was applied to both models.

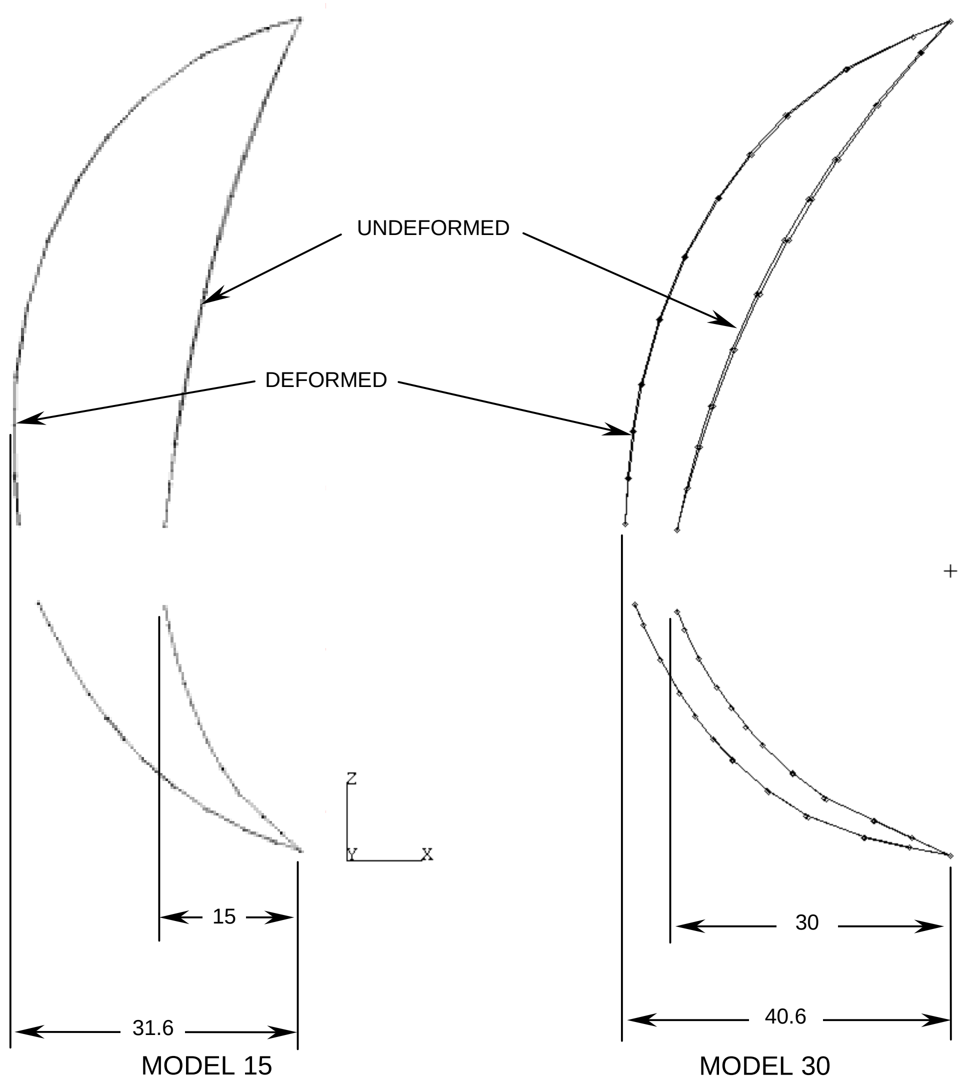

Figure 14. Influence of Initial deflection

As expected, the distance between the top of the deformed net and the plane of the fittings was larger for MODEL 30, but the deflection was higher for MODEL 15. The angle between the radial straps of the deformed net and the longitudinal axis was bigger for the model with the smaller initial deflection, resulting in higher radial components of the fitting reactions. If such an adjustment is possible, it would be beneficial to increase the initial deflection of the cargo net.

INFLUENCE OF LOADING CONDITIONS

To asses the influence of applied loads on the net deformed shape the three load cases described in the previous section were considered: (a) uniform pressure, (b) constant direction force parallel with the aircraft longitudinal axis, and (c) combination of uniform pressure and longitudinal force.

Figure 15 and Table 3 show little difference between the maximum deflection of the cargo net, but the angle between the radial straps and the fuselage longitudinal axis varies significantly. This is important for the attachment fittings, because the radial components of the reactions are more critical.

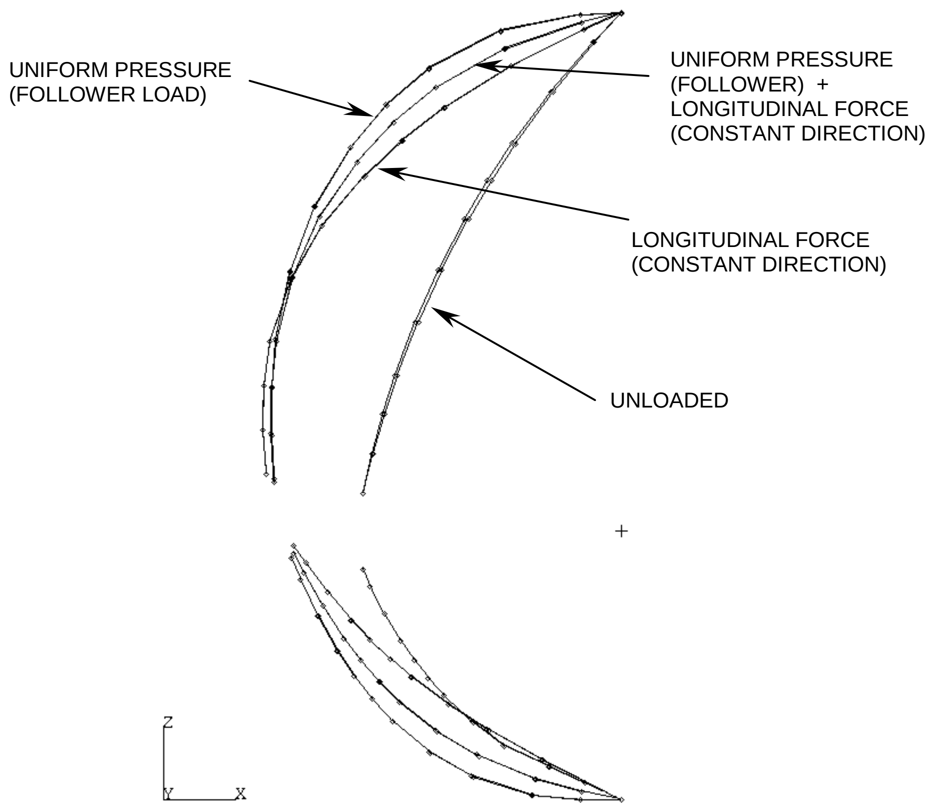

Figure 15. Influence of Applied Loads

Load Case	Max Deformation (%)
Longitudinal Force	100.
Uniform Pressure	96.1
Combination	96.3

Table 3. Influence of Applied Loads on Maximum Deformation

Under uniform pressure the radial straps are almost aligned with the longitudinal axis, resulting in lower radial components of the fuselage reactions. When the longitudinal force was applied, the angle between the radial straps and the aircraft longitudinal axis is greater. This is the most unfavorable configuration for the attachment fittings. The combination of uniform pressure and longitudinal forces falls in between the two extremes.

The angle between the radial straps and the longitudinal axis affects the magnitude and direction of the attachment fitting reactions. This is apparent especially for the radial components of the fuselage fitting reactions (Figure 16).

The radial components of the floor fitting reactions are not affected as much because the floor straps make an angle with both the longitudinal axis and the longitudinal vertical plane (Figure 17). The radial component due to the angle with the longitudinal vertical plane was almost unaffected by the different load cases.

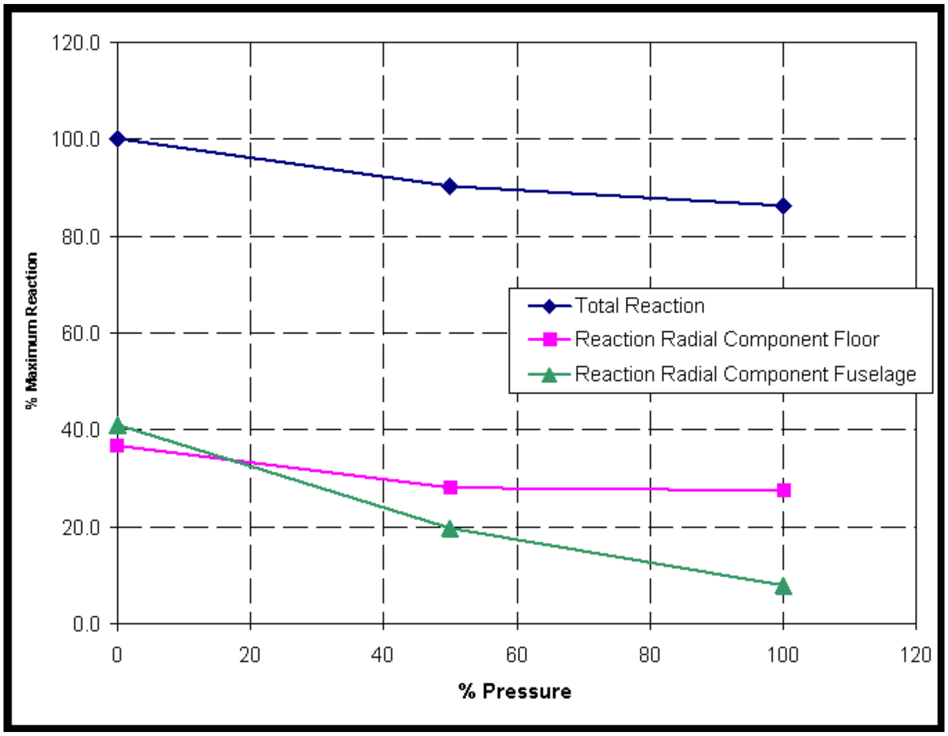

Figure 16. Influence of Loading Conditions

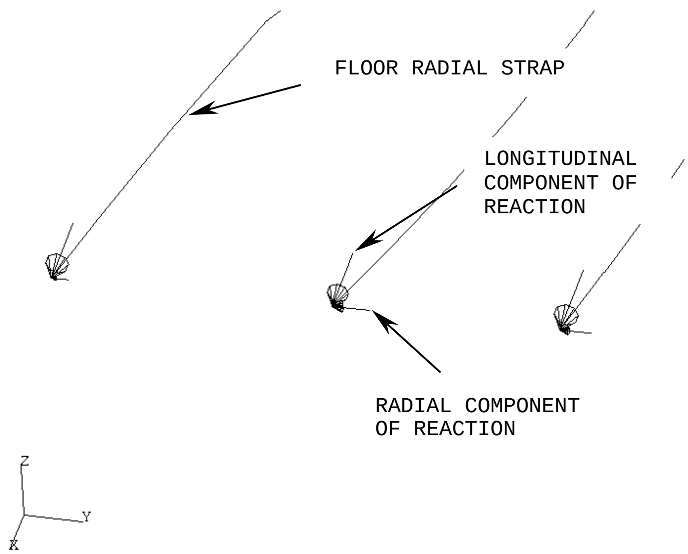

Figure 17. Radial Components of Floor Reactions

While it is impossible to know the exact make up of the cargo being carried, it appears the actual case is bracketed between the uniform pressure and the longitudinal force. The uniform pressure could be unconservative, while the longitudinal force is conservative. A combination of longitudinal force and uniform pressure will be closer to the real situation, but for stress check purposes the conservative approach should be used.

CONCLUSIONS

The modeling techniques and analysis strategies described in this paper should be useful to MSC/NASTRAN users that must solve similar problems. The most difficult issue was the model instability at the beginning of the load cycle due to the extreme flexibility of the unloaded cargo net. To achieve convergence the load for the first subcase was seven orders of magnitude lower than the final one.

The convergence criteria were relaxed during the first subcases while the shape of the net came closer to its equilibrium position. When equilibrium was achieved, the model stabilized and converged without problems, allowing the convergence criteria to be reset. Due to the net flexibility it is impossible to know the exact net shape before the impact. For a given length of the radial straps, the initial shape does not significantly influence the results.

The length of the radial straps determines the initial deflection of the net. This has a greater influence on the net extension and fitting reactions. If this parameter can be increased without exceeding the allowable net deflection, the maximum fitting reactions will be lower because of their more uniform distribution among the attachment points.

The influence of the cargo make up was investigated by considering three load cases. The uniform pressure is representative of a cargo comprising small and crushable parcels, while the force parallel with the aircraft longitudinal axis models the impact of a hard and heavy object. A combination of longitudinal forces and uniform pressure is expected to be closer to typical cargo loading, but for initial evaluations the longitudinal force is suggested for use since it is more conservative.

LIST OF ABBREVIATIONS AND SYMBOLS

DOF	Degree Of Freedom
FEA	Finite Element Analysis
FEM	Finite Element Model

REFERENCES

1. 14CFR25.561, Code of Federal Regulations, Title 14--Aeronautics And Space, Part 25--Airworthiness Standards: Transport Category Airplanes, Subpart C--Structure, Rev. January 1, 1998
2. *MSC/NASTRAN Version 70 Quick Reference Guide,* The MacNeal-Schwendler Corporation, Los Angeles, CA 1997
3. *MSC/NASTRAN Version 68 Reference Manual,* The MacNeal-Schwendler Corporation, Los Angeles, CA 1995